

Therapeutic targeting of endoplasmic reticulum stress in acute graft-versus-host disease

Eileen Haring,^{1,2,3} Geoffroy Andrieux,^{3,4} Franziska M. Uhl,^{1,2} Máté Krausz,⁵ Michele Proietti,⁵ Barbara Sauer,¹ Philipp R. Esser,⁶ Stefan F. Martin,⁶ Dietmar Pfeifer,¹ Annette Schmitt-Graeff,⁷ Justus Duyster,¹ Natalie Köhler,^{1,8} Bodo Grimbacher,^{5,8,9,10} Melanie Boerries,^{3,4,11} Konrad Aumann,¹² Robert Zeiser^{1,4,8} and Petya Apostolova^{1,3}

¹Department of Medicine I, Medical Center - Faculty of Medicine, University of Freiburg, Freiburg; ²Faculty of Biology, Albert-Ludwigs-University, Freiburg; ³German Cancer Consortium (DKTK), Partner site Freiburg and German Cancer Research Center (DKFZ), Heidelberg;

⁴Institute of Medical Bioinformatics and Systems Medicine, Medical Center - Faculty of Medicine, University of Freiburg, Freiburg; ⁵Institute for Immunodeficiency, Center for Chronic Immunodeficiency (CCI), Medical Center, Faculty of Medicine, Albert-Ludwigs-University, Freiburg; ⁶Allergy Research Group, Department of Dermatology, Medical Center - Faculty of Medicine, University of Freiburg, Freiburg; ⁷University of Freiburg, Freiburg; ⁸CIBSS - Center for Integrative Biological Signalling Studies, University of Freiburg, Freiburg; ⁹DZIF - German Center for Infection Research, Satellite Center Freiburg, Freiburg; ¹⁰RESIST - Cluster of Excellence 2155 to Hannover Medical School, Satellite Center Freiburg, Freiburg;

¹¹Comprehensive Cancer Center Freiburg (CCCF), Medical Center - Faculty of Medicine, University of Freiburg, Freiburg, and ¹²Department of Pathology, Medical Center - University of Freiburg, Faculty of Medicine, University of Freiburg, Freiburg, Germany

Correspondence:

Petya Apostolova
petya.apostolova@uniklinik-freiburg.de

Received: January 17, 2021.


Accepted: August 6, 2021.

Prepublished: August 19, 2021.

<https://doi.org/10.3324/haematol.2021.278387>

©2022 Ferrata Storti Foundation

Haematologica material is published under a CC

BY-NC license 

Abstract

Acute graft-versus-host disease (GvHD) is a life-threatening complication of allogeneic hematopoietic cell transplantation (allo-HCT), a potentially curative treatment for leukemia. Endoplasmic reticulum (ER) stress occurs when the protein folding capacity of the ER is oversaturated. How ER stress modulates tissue homeostasis in the context of alloimmunity is not well understood. We show that ER stress contributes to intestinal tissue injury during GvHD and can be targeted pharmacologically. We observed high levels of ER stress upon GvHD onset in a murine allo-HCT model and in human biopsies. These levels correlated with GvHD severity, underscoring a novel therapeutic potential. Elevated ER stress resulted in increased cell death of intestinal organoids. In a conditional knockout model, deletion of the ER stress regulator transcription factor *Xbp1* in intestinal epithelial cells induced a general ER stress signaling disruption and aggravated GvHD lethality. This phenotype was mediated by changes in the production of antimicrobial peptides and the microbiome composition as well as activation of pro-apoptotic signaling. Inhibition of inositol-requiring enzyme 1 α (IRE1 α), the most conserved signaling branch in ER stress, reduced GvHD development in mice. IRE1 α blockade by the small molecule inhibitor 4 μ 8c improved intestinal cell viability, without impairing hematopoietic regeneration and T-cell activity against tumor cells. Our findings in patient samples and mice indicate that excessive ER stress propagates tissue injury during GvHD. Reducing ER stress could improve the outcome of patients suffering from GvHD.

Introduction

Acute graft-versus-host disease (GvHD) is a life-threatening complication of allogeneic hematopoietic cell transplantation (allo-HCT). In particular, GvHD of the gastrointestinal tract (GI-GvHD) remains one of the most frequent causes of allo-HCT-related morbidity and mortality.¹ GI-GvHD results from a complex multi-step cross-talk between extensive epithelial tissue damage in the patient and activation of the allo-reactive immune system

transferred with the donor graft.² Enterocytes are subjected to cellular stress and undergo apoptosis. As a result, patients can develop diarrhea, dehydration, intestinal bleeding, hypalbuminemia, and generalized infections.² Recently, it has been shown that GvHD is also associated with changes of the microbiome diversity and composition.³ Standard treatment for GI-GvHD consists of corticosteroids or other compounds that target immune cell activation.⁴ Several factors supporting intestinal repair mechanisms have been identified in pre-clinical studies,

including IL-22,^{5,6} R-spondin^{7,8} and glucagon-like peptide 2.⁹ Recently, we have demonstrated a protective role for bile acids, which reduce cytokine-mediated intestinal injury and decrease intestinal antigen presentation.¹⁰ These novel developments show as a proof-of-principle that local regulation of repair mechanisms and inflammation is a successful approach to treat GI-GvHD and possibly other inflammatory diseases of the intestine.

In this study, we set out to decipher the role of endoplasmic reticulum (ER) stress, a cellular stress reaction, in the context of GI-GvHD. ER stress occurs upon accumulation of unfolded proteins in the ER lumen which can result from hypoxia, tissue damage, or pathogen exposure. These unfolded proteins are sensed by three molecules in the ER membrane which activate signaling cascades, commonly known as the unfolded protein response (UPR).¹¹ The most conserved UPR transducer is the kinase inositol-requiring enzyme 1 α (IRE1 α). This kinase has a ribonuclease activity and splices the mRNA of the transcription factor X-box binding protein 1 (XBP1), which then translocates to the nucleus and regulates the expression of chaperones, foldases and enzymes for lipid metabolism.^{12,13} The two other UPR branches are mediated by the protein kinase RNA-like ER kinase (PERK) and the activating transcription factor 6 (ATF6).¹¹ Their downstream signaling cascades lead to a reduction of the intracellular protein overload. The fundamental task of the UPR is to assist the cell in coping with the large amount of unfolded proteins. However, prolonged activation of the UPR also activates pro-apoptotic kinases and transcription factors.^{11,14,15} Another mechanism contributing to ER stress-induced cell death is mediated via regulated inositol-requiring enzyme 1-dependent decay of mRNA (RIDD).¹⁶ During this process, IRE1 α splices and thus inactivates multiple mRNA which results in cell death. These opposite effects of ER stress on cell fate underline the fact that a tight regulation of the UPR is necessary to maintain physiological balance and homeostasis in stressed cells (Figure 1A).

Our study aimed to close the gap in understanding the function of intestinal UPR and its therapeutic potential in GI-GvHD. We observed that ER stress occurred during GvHD development in mice and humans and correlated with GI-GvHD onset and severity. Using intestinal organoids and a genetic conditional knockout mouse model, we found that dysregulated chronic ER stress reduced intestinal cell viability and aggravated GvHD severity by altering anti-microbial peptide production, the microbiome composition and pro-apoptotic pathway activity. Pharmacological inhibition of IRE1 α , one of three ER stress signaling pathways, improved GvHD outcome by directly protecting the intestinal epithelium. Importantly, this intervention did not impair hematopoietic regeneration, T-cell proliferation or anti-tumor killing capacity.

Our study proposes the inhibition of this ER stress pathway as a novel approach for the treatment of GI-GvHD.

Methods

Mice

BALB/c (H-2K^d) and C57BL/6 (H-2K^b) mice were purchased from Janvier Labs (Le Genest-Saint-Isle, France). Luciferase-transgenic C57BL/6 mice (H-2K^b) were bred in the animal facility of the Center for Clinical Research at the Medical Center – University of Freiburg, Germany. Mice carrying a floxed *Xbp1* allele (*Xbp1*^{fl/fl}) have been previously described¹⁷ and were a kind gift from Dr. Laurie Glimcher, Cornell University, USA. B6. Cg-Tg(*Vil*^{1-cre})997Gum/J mice expressing the Cre recombinase in villus and crypt intestinal epithelial cells (*Vil*^{Cre}) were purchased from the Jackson Laboratory. *Vil*^{Cre}*Xbp1*^{fl/fl} mice and *Xbp1*^{fl/fl} littermates were generated by crossing these two strains. All animals were housed under specific pathogen-free conditions at the animal facility of the Center for Clinical Research (ZKF, Freiburg, Germany). Genotypes were confirmed via polymerase chain reaction (PCR). All animal protocols (G-16/018, G-17/063, G-18/063; X-13/07J; X-15/10A; X20/06K) were approved by the Federal Ministry for Nature, Environment and Consumer Protection of the state of Baden-Württemberg, Germany.

All other methods are provided in the *Online Supplementary Appendix*.

Results

Unfolded protein response is activated during early graft-versus-host disease development in mice

We first characterized the UPR activity in the intestine of healthy mice and after GvHD induction by quantifying the splicing of *Xbp1*, which is one of the initiating events of UPR signaling. We observed increased *Xbp1* splicing in the colon of mice 7 days after allo-HCT when compared to untreated mice (*Online Supplementary Figure S1A-C*). In order to study the exact time course of UPR activation, we performed quantification of the established ER stress markers *Xbp1s/Xbp1u* (spliced *Xbp1* in relation to unspliced *Xbp1*) and *Hspa5* (encoding for the chaperone GRP78, also known as BIP) at multiple time points after allo-HCT (Figure 1B). We further set out to distinguish whether ER stress was induced as a consequence of the conditioning treatment alone (total body irradiation [TBI]) or by the allo-immune reaction that marks GvHD development. We observed an upregulation of the UPR-related markers in the small intestine (*Online Supplementary Figure S1D*) and in the colon (Figure 1C) of both TBI and GvHD mice when compared to healthy mice. While ER stress markers were

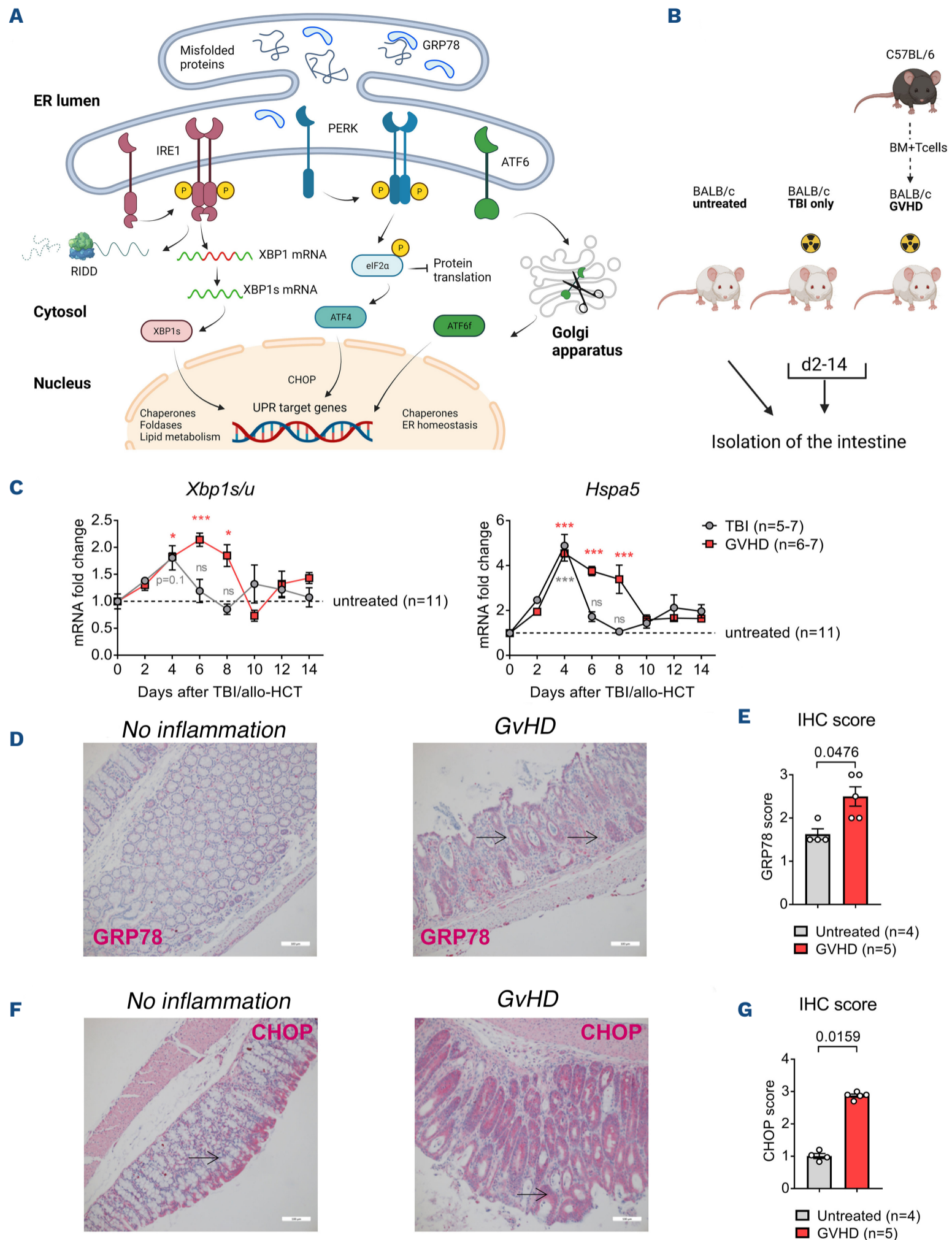


Figure 1. Graft-versus-host disease induction leads to endoplasmic reticulum stress in the murine intestine. (A) Schematic overview of the three different unfolded protein response (UPR) branches induced by endoplasmic reticulum (ER) stress, created with BioRender.com. (B, C) BALB/c mice received either only total body irradiation (TBI) with 10 Gy or underwent complete allogeneic hematopoietic cell transplantation (allo-HCT) as described in Methods with 5×10^6 bone marrow (BM) cells and 3×10^5 CD4⁺ and CD8⁺ T cells isolated from the spleen of a C57BL/6 donor. Untreated BALB/c mice were used as a control. (B) Overview of the experimental setup, created with BioRender.com. (C) Quantitative real-time polymerase chain reaction (PCR) analysis of the mRNA expression of selected UPR marker genes in the colon with *Actb* as a reference gene. Samples were isolated on different time points after TBI or allo-HCT as indicated. The dashed line represents the expression level in untreated mice, which

Continued on following page.

was set to 1. Data were pooled from $n=11$ mice for day 0 (d0) and $n=5-7$ mice/group for the other time points. The P -values were calculated using the ordinary one-way ANOVA with correction for multiple comparisons. Statistical comparisons between “GvHD” and “untreated” are highlighted in red color, statistical comparisons between “TBI” and “untreated” are highlighted in grey color, $*P<0.05$, $***P<0.0001$. (D) Representative immunohistochemistry staining images for GRP78 in murine colon tissue sections. Sections from an untreated mouse (“no inflammation”) and from an allo-transplanted BALB/c mouse (“GvHD”) on d7 after allo-HCT are shown. Arrows point to GRP78-expressing cells. Scale bars 100 μM . (E) Quantification of the GRP78 expression score. Each dot represents a single mouse, $n=4-5$ mice/group. The P -value was calculated using a two-tailed unpaired Mann Whitney U test. (F) Representative immunohistochemistry staining images for CHOP in murine colon tissue sections. Sections from an untreated mouse (“no inflammation”) and from an allo-transplanted BALB/c mouse (“GvHD”) on d7 after allo-HCT are shown. Arrows point to GRP78-expressing cells. Scale bars 100 μM . (G) Quantification of the CHOP expression score. Each dot represents a single mouse, $n=4-5$ mice/group. The P -value was calculated using a two-tailed unpaired Mann Whitney U test.

induced by TBI as early as day 4, they dropped back to normal more rapidly than in mice with GvHD. Especially 6-8 days after GvHD induction in our model, *Xbp1s/Xbp1u* and *Hspa5* expression were significantly higher in mice developing GvHD compared to TBI mice and healthy controls (Figure 1C). After that time point, ER stress levels in the colon declined and were similar to baseline (Figure 1C) whereas in the small intestine a second increase was observed on day 14 after allo-HCT (*Online Supplementary Figure S1D*). These data indicate an active UPR during early GI-GvHD development. While we observed that TBI alone can induce the UPR, transfer of T cells aggravated ER stress additionally. In line with this, immunohistochemistry for GRP78 showed increased expression in the colon of GvHD mice when compared to healthy colon tissue (Figure 1D to E). Although the aim of the UPR is to support the cellular survival in stress conditions by reducing the load of unfolded proteins, pro-apoptotic cascades are engaged during prolonged ER stress. C/EBP homologous protein (CHOP, encoded by the gene *Ddit3*) is one of the transcription factors mediating apoptosis in the context of the UPR. We found that CHOP is expressed by the healthy colonic epithelium, especially at the top of the crypts. Interestingly, the expression in GvHD-developing mice extended to the whole crypt (Figure 1F, G). As epithelial regeneration has its origin at the bottom of the crypts where intestinal stem cells reside, CHOP-induced apoptosis in this area might reduce the capacity of the intestine to regenerate itself. Together, we observed that GI-GvHD development in mice is marked by increased levels of ER stress.

Unfolded protein response is activated during graft-versus-host disease (GvHD) onset in humans and correlates with GvHD severity

GI-GvHD is a major factor contributing to morbidity and mortality in allo-HCT recipients. In order to assess whether the UPR was activated in humans, we examined biopsies of GvHD patients for the expression of GRP78 and CHOP. Healthy tissue and biopsies from colitis patients were used as negative and positive controls, respectively. In the uninflamed intestine, expression of GRP78 was confined to immune cells that were interspersed between

crypts, and staining in epithelial cells was low (Figure 2A). Confirming a previously shown connection between ER stress and colitis,¹⁷ GRP78 expression in the epithelium was strong in colitis samples. When analyzing biopsies from GvHD patients, we observed increased expression in higher-grade GvHD compared to lower-grade GvHD (Figure 2A and B). Similarly, healthy colon tissue showed only low expression of CHOP. We observed a more intensive CHOP signal in biopsies from patients with GvHD grade 2-3, especially from injured crypts that were undergoing cell death (Figure 2C). Histology data were supported by the analysis of a publicly available RNA sequencing data set (GSE134662), generated by Holtan *et al.*¹⁸ We found an up-regulation of various ER stress-related genes when comparing gut biopsies from newly diagnosed or steroid-refractory GvHD to healthy tissue (*Online Supplementary Figure S2A, B*). Gene set enrichment analysis confirmed a differential expression of genes matched to the GO term “Response to endoplasmic reticulum stress” (*Online Supplementary Figure S2C*). Collectively, our data show that ER stress occurs during GvHD development in mice and humans, and that its levels correlate with GvHD severity.

Chronic endoplasmic reticulum stress aggravates intestinal cell death and graft-versus-host disease

Based on our observation that the UPR is activated during GvHD, we investigated the cellular impact of ER stress induction on the intestine using murine small intestinal organoids that were established and cultured as previously described.¹⁹ Exposure of organoids to the ER stress inducer tunicamycin resulted in cell death as observed by microscopy and flow cytometry (Figure 3A-D). Release of DAMP from dying cells contributes to the activation of antigen-presenting cells in the context of GvHD.^{20,21} We detected increased concentrations of the DAMP uric acid in the supernatants of tunicamycin-treated organoids (Figure 3E). Next, we investigated if UPR pathway disruption affects GvHD outcome in a murine allo-HCT model. Since the IRE1 α pathway is the most conserved branch among different species, we focused on the key transcription factor XBP1 which is downstream of IRE1 α and gets activated by the RNase activity of this enzyme. In order to test whether

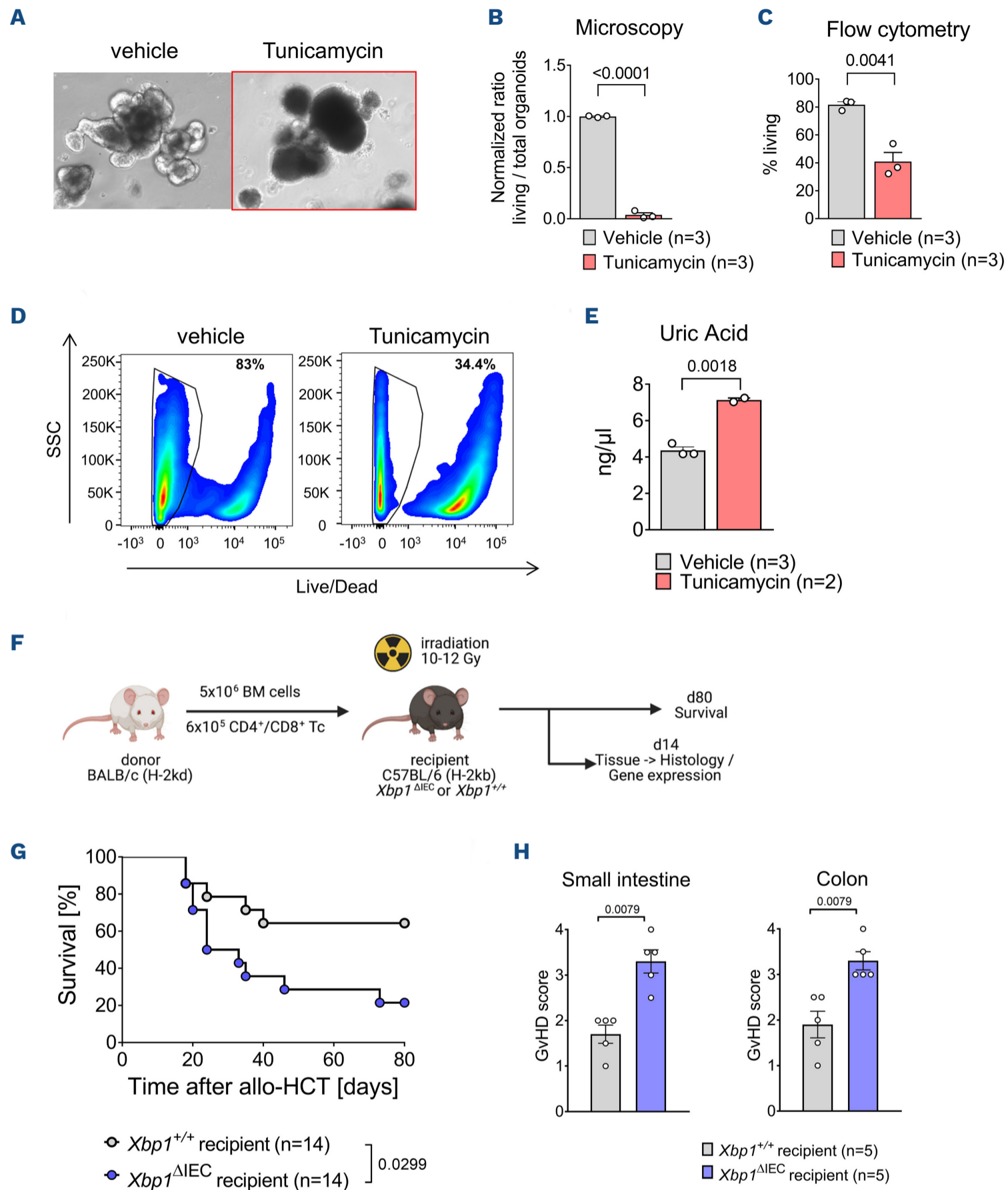


Figure 3. Chronic endoplasmic reticulum stress induces intestinal cell death and a more severe graft-versus-host disease phenotype. (A) Representative images of BALB/c intestinal organoids treated for 24 hours (h) with 1 μ g/mL tunicamycin or vehicle control. (B) Quantification of living organoids after vehicle or tunicamycin treatment as in (A) performed by manual microscope counting. Data were normalized to the vehicle group. Statistical analysis of $n=3$ biologically independent experiments. The P -value was calculated using the two-tailed unpaired Student's t -test. (C, D) Intestinal organoids were cultured as described in (A). Organoids were digested and the proportion of dead cells was determined by flow cytometry. (C) Quantification of the percentage of dead cells. The P -value was calculated using the two-tailed unpaired Student's t -test. (D) Representative flow cytometry dot plots. (E) Organoids were treated with 0.15 μ g/mL tunicamycin for 12 h and afterwards allowed to rest for further 24 h in normal medium. Levels of uric acid were measured in the supernatant medium, in which the organoids were rested. Concentrations were measured in total ng/ μ L, $n=2-3$ individual biological replicates/group. The P -value was calculated using the two-tailed unpaired Student's t -test. (F) Transplantation model with BALB/c (H-2Kd) as donor and *Xbp1* $^{\Delta\text{IEC}}$ or *Xbp1* $^{+/+}$ mice as recipients, created with Biorender.com. (G) Survival of *Xbp1* $^{\Delta\text{IEC}}$ and *Xbp1* $^{+/+}$ mice after allogeneic hematopoietic cell transplantation (allo-HCT). Data were pooled from three independent experiments with $n=14$ mice/group. The P -value was calculated using the two-sided Mantel-Cox test. (H) Histopathology scores of the small intestine and colon from *Xbp1* $^{\Delta\text{IEC}}$ and *Xbp1* $^{+/+}$ recipients on day 14 after allo-HCT. Data are pooled from $n=5$ mice/group. Each dot represents a single mouse. The P -values were calculated using the two-tailed unpaired Mann Whitney U test.

were downregulated in *Xbp1^{ΔIEC}* mice with GvHD when compared to littermate controls (Figure 4A). Amongst these were *Defa1*, *Defa5*, *Defa20*, *Defa21*, *Defa22*, *Defa30*, *Defa34*, *Defa39*, and *Defa41*. Defensins are anti-microbial peptides, secreted by Paneth cells. A decrease in defensin gene expression is in line with previously reported loss of Paneth cells in *Xbp1^{ΔIEC}* mice.¹⁷ We next explored how the expression of anti-microbial peptides varied during GvHD development. We observed reduced mRNA expression of *Defa1*, *Defa4*, lysozyme (*Lyz*) and regenerating islet-derived protein 3γ (*Reg3g*) in untreated *Xbp1^{ΔIEC}* mice compared to *Xbp1^{+/+}* littermates. GvHD induction reduced initially the expression of all four genes (Figure 4B). On day 14 after allo-HCT, anti-microbial peptide expression in *Xbp1^{+/+}* mice had returned to normal levels whereas it stayed significantly lower in *Xbp1^{ΔIEC}* mice (Figure 4B).

Previous studies have suggested that the intestinal dysbiosis, which is frequently observed in GvHD, results at least in part from the reduction of Paneth cells and their products in intestinal crypts.²² We hypothesized that reduced anti-microbial peptide expression in *Xbp1^{ΔIEC}* animals might be accompanied by changes in the microbiome. We analyzed the microbiome of *Xbp1^{ΔIEC}* and *Xbp1^{+/+}* control mice with or without GvHD induction. We observed changes on the phylum level in the untreated condition with a shift towards more Bacteroidetes and less Firmicutes in *Xbp1^{ΔIEC}* mice (Figure 4C, D). Loss of Firmicutes, and specifically some *Clostridia* species has previously been linked to GvHD.²³ We found that within the Firmicutes phylum, the *Clostridia* class was particularly reduced with decreased abundances of the families Ruminococcaceae and Lachnospiraceae in *Xbp1^{ΔIEC}* mice (Figure 4E), the latter of which has been associated with a protective effect against lethal GvHD.^{24,25} In the early phase after allo-HCT, there were no differences in the microbiome composition between *Xbp1^{+/+}* and *Xbp1^{ΔIEC}* mice (Figure 4C, D), mirroring the comparable levels of anti-microbial peptides that we observed at this time point (Figure 4B). These data indicate that ER stress signaling dysregulation caused by loss of *Xbp1* induces a loss of anti-microbial peptides, coinciding with a shift in the microbiome composition in the steady-state that is equivalent to the microbiome disruption during lethal GvHD development.

Loss of *Xbp1* promotes a shift towards pro-apoptotic unfolded protein response signaling which can be reversed by a pharmacological intervention

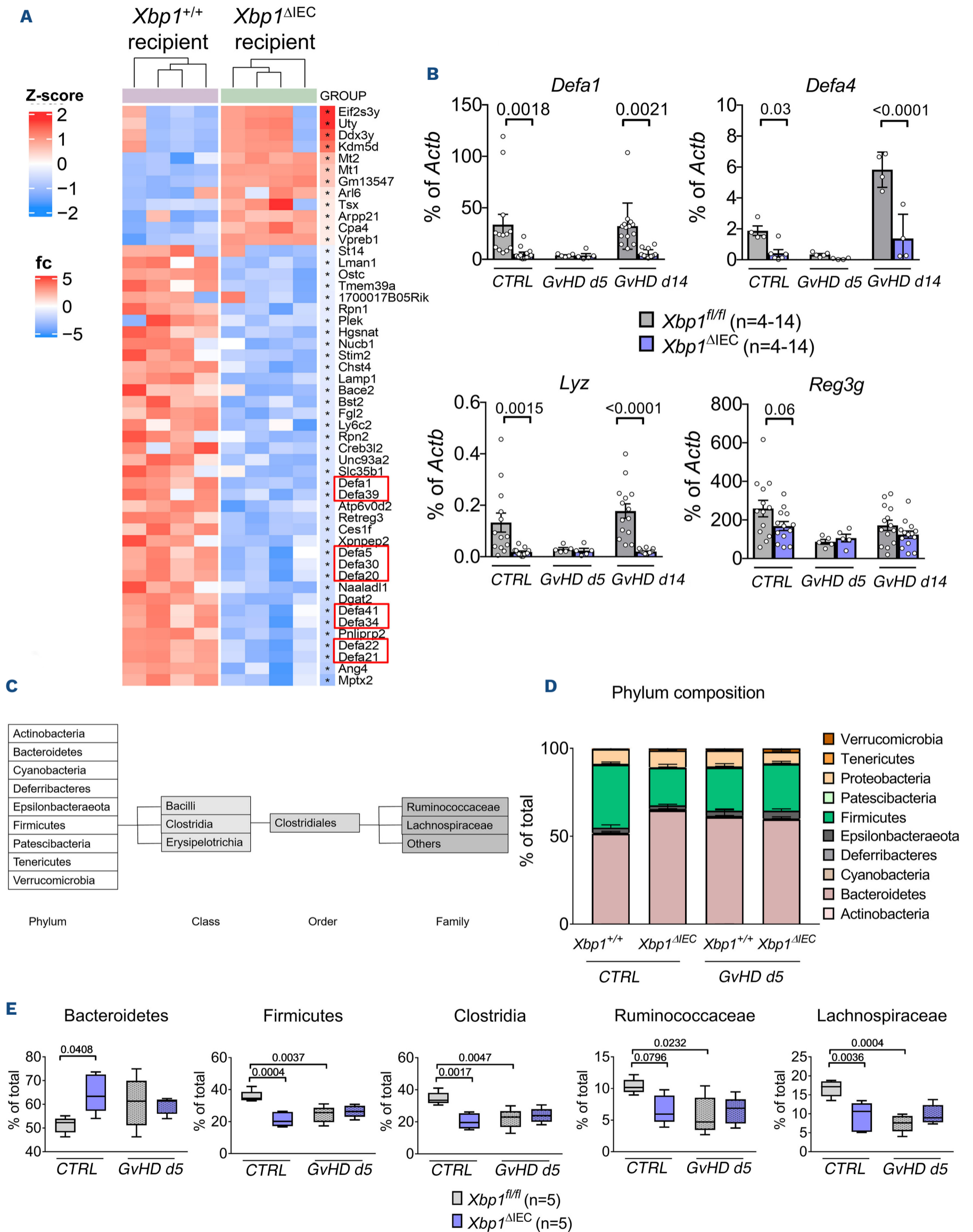
We further hypothesized that the observed aggravated GvHD phenotype might be caused by upregulation of pro-apoptotic UPR signaling in *Xbp1^{ΔIEC}* mice. RIDD is an IRE1α-dependent process that gets activated upon prolonged ER stress. IRE1α RNase activity cleaves several mRNA with subsequent apoptosis induction. We observed signifi-

cantly decreased levels of the RIDD targets bone marrow stromal cell antigen 2 (*Bst2*), lysosomal-associated membrane protein 1 (*Lamp1*), carboxylesterase 1F (*Ces1f*), solute carrier family 35, member B1 (*Slc35b1*), ribophorin II (*Rpn2*) and heparan-α-glucosamide N-acetyltransferase (*Hgsnat*) in the intestine of *Xbp1^{ΔIEC}* recipient mice (Figure 4A; Figure 5A, B). Consistent with the hypothesis that *Xbp1* deletion favors other, pro-apoptotic ER stress branches, *Ddit3*, encoding for CHOP, was upregulated (Figure 5C). We then explored the question of whether compensatory over-activation of IRE1α-related RIDD mediates the aggravated GvHD phenotype in mice with intestinal *Xbp1* deletion. We employed a small molecule inhibitor of IRE1α, 4μ8c (7-hydroxy-4-methyl-2-oxo-2H-1-benzopyran-8-carboxaldehyde). This compound blocks the RNase activity of IRE1α, including RIDD, but spares its kinase activity. We observed that treatment of *Xbp1^{ΔIEC}* mice with 4μ8c restored the survival upon GvHD induction to the level observed in *Xbp1^{+/+}* littermates (Figure 5D). Taken together, we show that selective inactivation of intestinal *Xbp1* results in a major dysregulation of the UPR with a pro-apoptotic signature.

Inhibition of IRE1α improves graft-versus-host disease outcome without impairing immune reconstitution or the graft-versus-leukemia effect

We observed that inhibition of IRE1α reverses the toxicity of chronic ER stress in *Xbp1^{ΔIEC}* mice and therefore studied the potential of the IRE1α inhibitor as a therapeutic compound for general GvHD development and outcome. *In vivo* treatment of mice who had developed GvHD with the IRE1α inhibitor 4μ8c ameliorated GvHD severity, as observed by prolonged survival, reduced clinical GvHD signs and decreased histopathology score (Figure 6A, D). A beneficial effect, albeit not as strong as with 4μ8c, was observed with a second IRE1α inhibitor, B-109 (*Online Supplementary Figure S4A*). On the contrary, inhibition of PERK signaling did not improve the GvHD outcome (*Online Supplementary Figure S4B*). Given the beneficial effect of IRE1α inhibition over PERK inhibition, we focused on the effects of the former pathway in our further analysis. In line with the hypothesis that inhibition of IRE1α reduces GvHD-related intestinal apoptosis, 4μ8c decreased intestinal cell death in response to treatment with the pro-inflammatory cytokine TNF or the ER stress inducer tunicamycin *in vitro* in the small intestinal cell line MODE-K (Figure 6E, G).

Long-term success of allo-HCT strongly depends on an intact immune reconstitution that guarantees protection against pathogens and malignancy relapse. We therefore next analyzed whether IRE1α inhibition had an impact on peripheral blood leukocyte and thymus regeneration (Figure 7A). We found that, as expected, hemoglobin, platelets and white blood cells were significantly decreased in the



Continued on following page.

Figure 4. The deletion of intestinal *Xbp1* disrupts antimicrobial peptide production and induces changes in the microbiome. (D) Heatmap showing the top 50 differentially expressed genes in the small intestine of *Xbp1*^{ΔIEC} and *Xbp1*^{+/+} recipient mice on day 14 after allogeneic hematopoietic cell transplantation (allo-HCT) performed as shown in Figure 3F. Color legend “Z-score” indicates the row-wise scaling of the normalized intensity, whereas “fc” indicates the log₂ fold change between *Xbp1*^{+/+} and *Xbp1*^{ΔIEC} recipient mice. (B) Quantitative real-time polymerase chain reaction (PCR) analysis of the mRNA expression of the antimicrobial peptides *Defa1*, *Defa4*, *Lyz* and *Reg3g* in the indicated groups with *Actb* as a reference gene. Data were pooled from n=5-14 mice/group. Each dot represents a single mouse. The *P*-values were calculated using the ordinary one-way ANOVA with correction for multiple comparisons. (C) Simplified overview of bacteria taxonomy with a focus on the phylum *Firmicutes*. (D, E) Microbiome analysis of untreated (CTRL) and graft-versus-host disease (GVHD)-developing *Xbp1*^{ΔIEC} and *Xbp1*^{+/+} mice on day 5 after allo-HCT. Data were pooled from n=5 independent biological replicates. The *P*-values were calculated using an ordinary one-way ANOVA with correction for multiple comparisons. (D) Phylum composition. (E) Relative abundance of the phyla Bacteroidetes and Firmicutes, the class Clostridia and the families Ruminococcaceae and Lachnospiraceae.

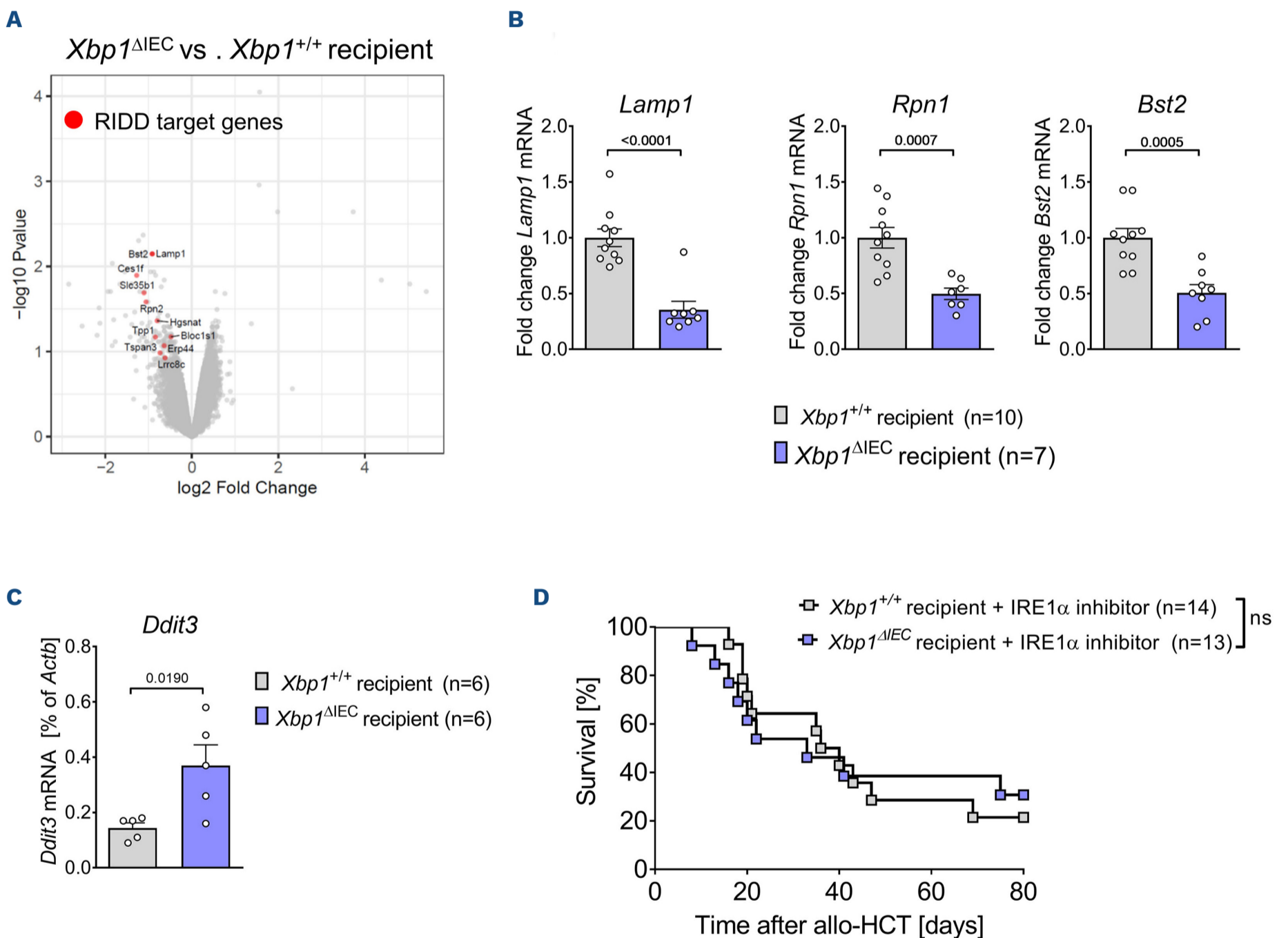
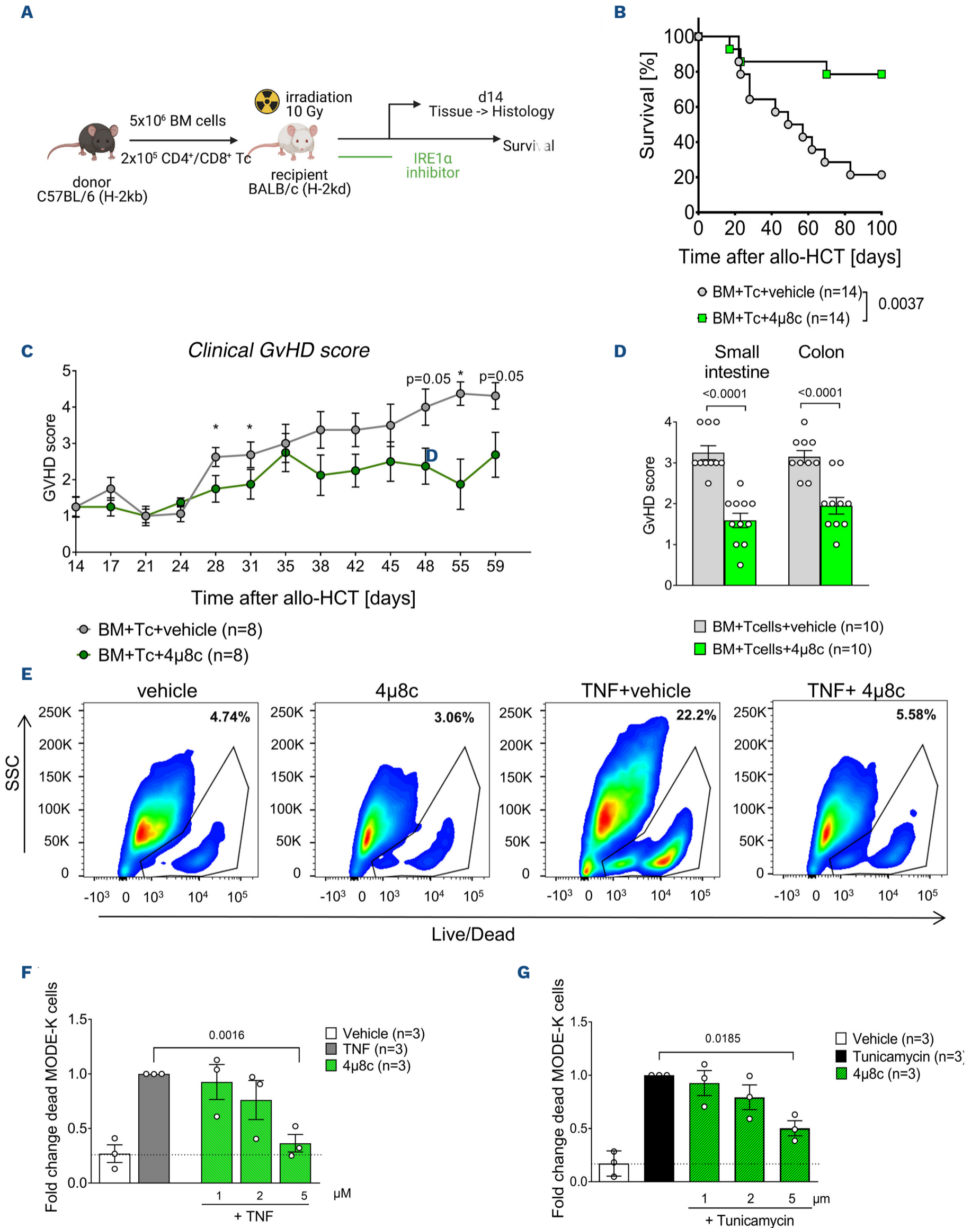


Figure 5. Loss of *Xbp1* favors pro-apoptotic signaling. (A-D) *Xbp1*^{ΔIEC} and *Xbp1*^{+/+} mice underwent bone marrow transplantation (BMT) as in Figure 3F. (A) Volcano plot showing gene expression in *Xbp1*^{ΔIEC} vs. *Xbp1*^{+/+} recipient mice on day 14 after allogeneic hematopoietic cell transplantation (allo-HCT). Red circles highlight mRNA that are targets of RIDD. (B) Quantitative real-time polymerase chain reaction (PCR) analysis of the mRNA expression of the RIDD target genes *Lamp1*, *Rpn1* and *Bst2* in the indicated groups with *Actb* as a reference gene. Data were pooled from n=10 mice in the *Xbp1*^{+/+} group and n=7 mice in the *Xbp1*^{ΔIEC} group. Each dot represents a single mouse. *P*-values were calculated using the two-tailed unpaired Student’s *t*-test. (C) Quantitative real-time PCR analysis of the mRNA expression of the pro-apoptotic endoplasmic reticulum (ER) stress gene *Ddit3* (encodes for CHOP) with *Actb* as a reference gene. Data were pooled from n=6 mice/group. Each dot represents a single mouse. *P*-values were calculated using the two-tailed unpaired Student’s *t*-test. (D) Survival of *Xbp1*^{ΔIEC} and *Xbp1*^{+/+} mice after allo-HCT and treatment with the IRE1α inhibitor 4μ8c. Data were pooled from three independent experiments with n=13-14 mice/group. Each dot represents a single mouse. *P*-values were calculated using the two-sided Mantel-Cox test.



Continued on following page.

Figure 6. Pharmacological IRE1 α inhibition improves graft-versus-host disease outcome in mice. (A) Transplantation model with C57BL/6 (H-2K^b) as donor and BALB/c (H-2K^d) as recipient. Recipient animals were treated with 10 mg/kg body weight IRE1 α inhibitor 4 μ 8c (from day 0 until day 10 after bone marrow transplantation [BMT]) or an equal volume of vehicle by a daily intraperitoneal (i.p.) injection. Schematic overview created with BioRender.com. (B) Survival of BALB/c mice transplanted and treated with 4 μ 8c as shown in (A). Data were pooled from two independent experiments, n=14 mice/group. The *P*-value was calculated using the two-sided Mantel-Cox test. (C) Clinical graft-versus-host disease (GvHD) scores combined from weight loss, skin lesions, hunching posture, dull fur and diarrhea in BALB/c mice transplanted as shown in (A). Data were pooled from n=8 mice/group. The *P*-values were calculated using the two-tailed unpaired Mann-Whitney U test. (D) Histopathology scores of the small intestine and colon from BALB/c mice transplanted and treated as in (A) on day 14 after allogeneic hematopoietic cell transplantation (allo-HCT). Data are pooled from n=7 (BM+vehicle group) and n=10 mice (BM+Tcell+vehicle and BM+Tcell+4 μ 8c groups). *P*-values were calculated using the two-tailed unpaired Mann-Whitney U test. (E, F) Analysis of MODE-K cell viability after treatment with TNF (20 ng/mL) \pm 4 μ 8c (concentrations as indicated) for 48 hours (h) performed by flow cytometry. (E) Representative flow cytometry dot plots. (F) Quantification of the percentages of dead cells. Data were normalized to the TNF-treated group. Statistical analysis of n=3 biologically independent experiments performed in technical duplicates or triplicates. The *P*-values were calculated using the ordinary one-way ANOVA test. (G) Analysis of MODE-K cell viability after treatment with 0.15 μ g/mL tunicamycin \pm 4 μ 8c (concentrations as indicated) for 48 hours. Quantification of the percentages of dead cells. Statistical analysis of n=3 independent experiments each performed in technical triplicates. Data were normalized to the tunicamycin treatment group. The *P*-values were calculated using the ordinary one-way ANOVA test.

blood of mice on day 14 after allo-HCT when compared to untreated mice. By day 29, hemoglobin and platelets had recovered to normal levels, whereas the white blood cells, and specifically B and T lymphocytes remained reduced by about 80% (Figure 7B, C). Importantly, there was no difference between vehicle- and 4 μ 8c-treated animals (Figure 7B, C). Peripheral blood T-cell differentiation into naïve, effector and central memory T cells was also not affected by IRE1 α inhibition (*Online Supplementary Figure S5A*). Thymus pathology following TBI and GvHD development can impair the T-cell selection process leading to the emergence of an autoreactive population and a failure to generate functional T cells that fight cancer cells and pathogens. Analysis of the thymic T cell populations showed that, independently of 4 μ 8c treatment, CD4⁺ CD8⁺ double positive (DP), that are the most frequent population in the healthy thymus, represent only 8% of the cells in allo-HCT recipients. In the same time, the single positive CD4⁺ population had expanded to 72% (Figure 7D) after allo-HCT. In the non-hematopoietic compartment, we observed no changes in the percentages of thymus epithelial cells or fibroblasts in 4 μ 8c- compared to vehicle-treated animals (Figure 7E). Overall, these data provide evidence that hematopoietic and thymus regeneration is not affected by administration of 4 μ 8c to d29, although long-term studies of lymphocyte regeneration and thymic populations would be required to provide definitive confirmation.

Long-term malignancy control by allo-reactive T cells is essential for the success of allo-HCT. We assessed the expansion of allo-reactive T cells by bioluminescence imaging and flow cytometry and found that 4 μ 8c did not impact T-cell expansion and differentiation *in vivo* (Figure 8A-D). We next tested whether IRE1 α inhibition interfered with the graft-versus-tumor effect. We activated T cells *via* co-culture with allogeneic bone marrow-derived dendritic cells in the presence or absence of 4 μ 8c. After 72 hours of activation, the T cells were incubated

with A20 lymphoma cells and the killing efficacy was evaluated by flow cytometry (Figure 8E). We observed a similar capacity of vehicle- and 4 μ 8c-pretreated T cells to eliminate A20 cells (Figure 8F). Collectively, these data show that pharmacological inhibition of IRE1 α does not impair the killing capacity of allo-reactive T cells.

Discussion

Acute GvHD affects about 50% of allo-HCT recipients with more than 10% of all patients suffering from a severe course of the disease.¹ Recent efforts to improve the efficacy of treatment and prophylaxis range from blockade of T-cell activation,^{26,27} to inhibition of cytokine signaling^{28,29} and epigenetic therapies.³⁰

In this study, we hypothesized that intestinal ER stress could be a target for novel GvHD therapies. We observed an upregulation of multiple ER stress markers following irradiation and GvHD induction. This is in line with a previous report showing upregulation of chaperones after allogeneic transplantation.³¹ Upregulation of ER stress markers has also been observed in the lacrimal gland, small intestine, skin and liver of mice developing chronic GvHD.³² In an extended analysis of a publicly available RNA sequencing data set (GSE134662),¹⁸ we found increased expression of several UPR genes in human GvHD samples compared to healthy tissue. Furthermore, we found that the expression of two ER stress markers, GRP78 and CHOP, directly correlated with GvHD severity in a cohort of patients at our center. The association of ER stress marker expression with higher-grade GvHD in patients strengthens the implication that modulation of intestinal UPR might be a successful treatment approach.

We next hypothesized that chronic unresolved ER stress might aggravate GvHD. We performed experiments using murine intestinal organoids as an *in vitro* model, and with a conditional knockout model of the transcription factor *Xbp1* *in vivo*. Induction of ER stress by a chemical compound in-

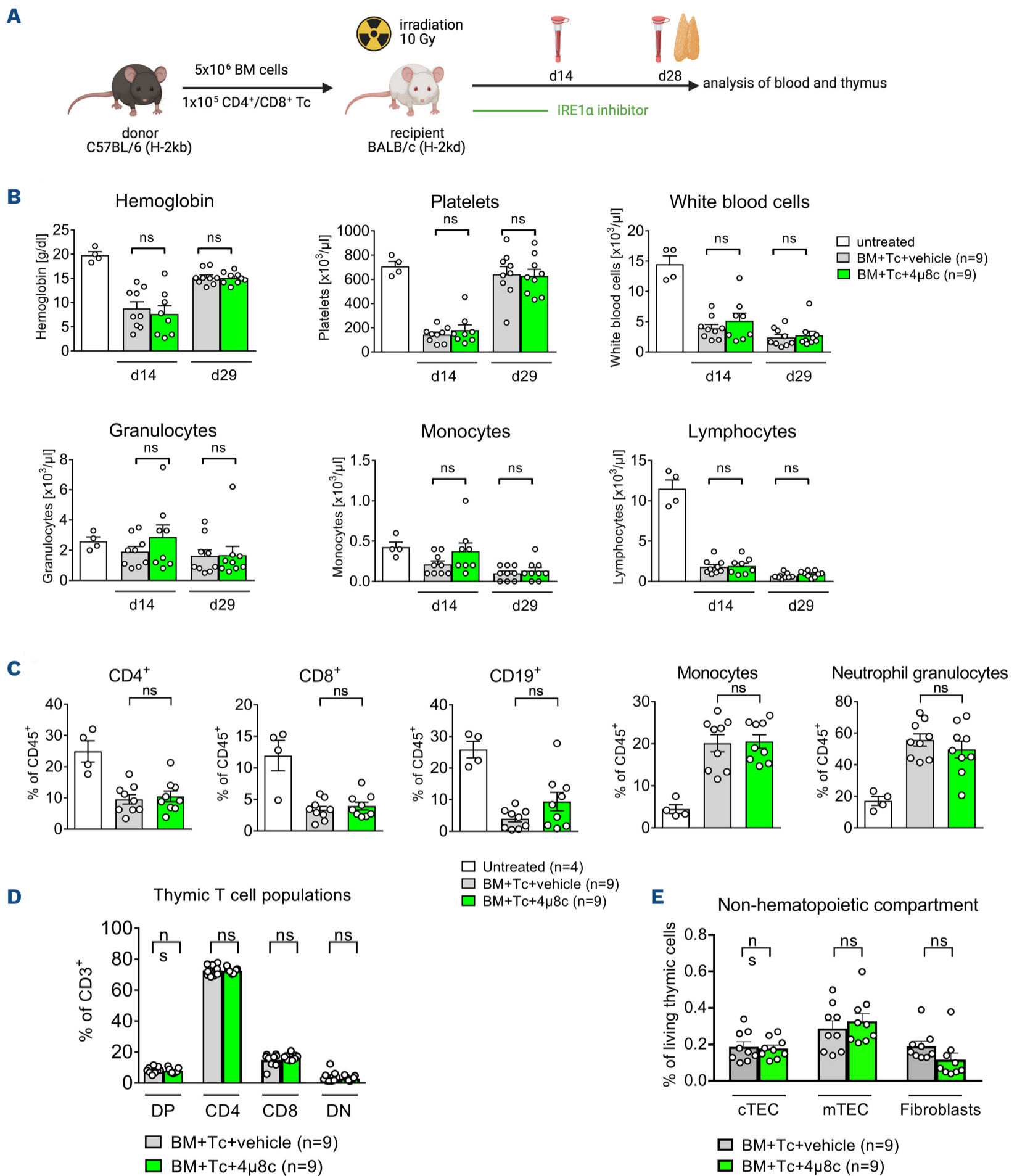
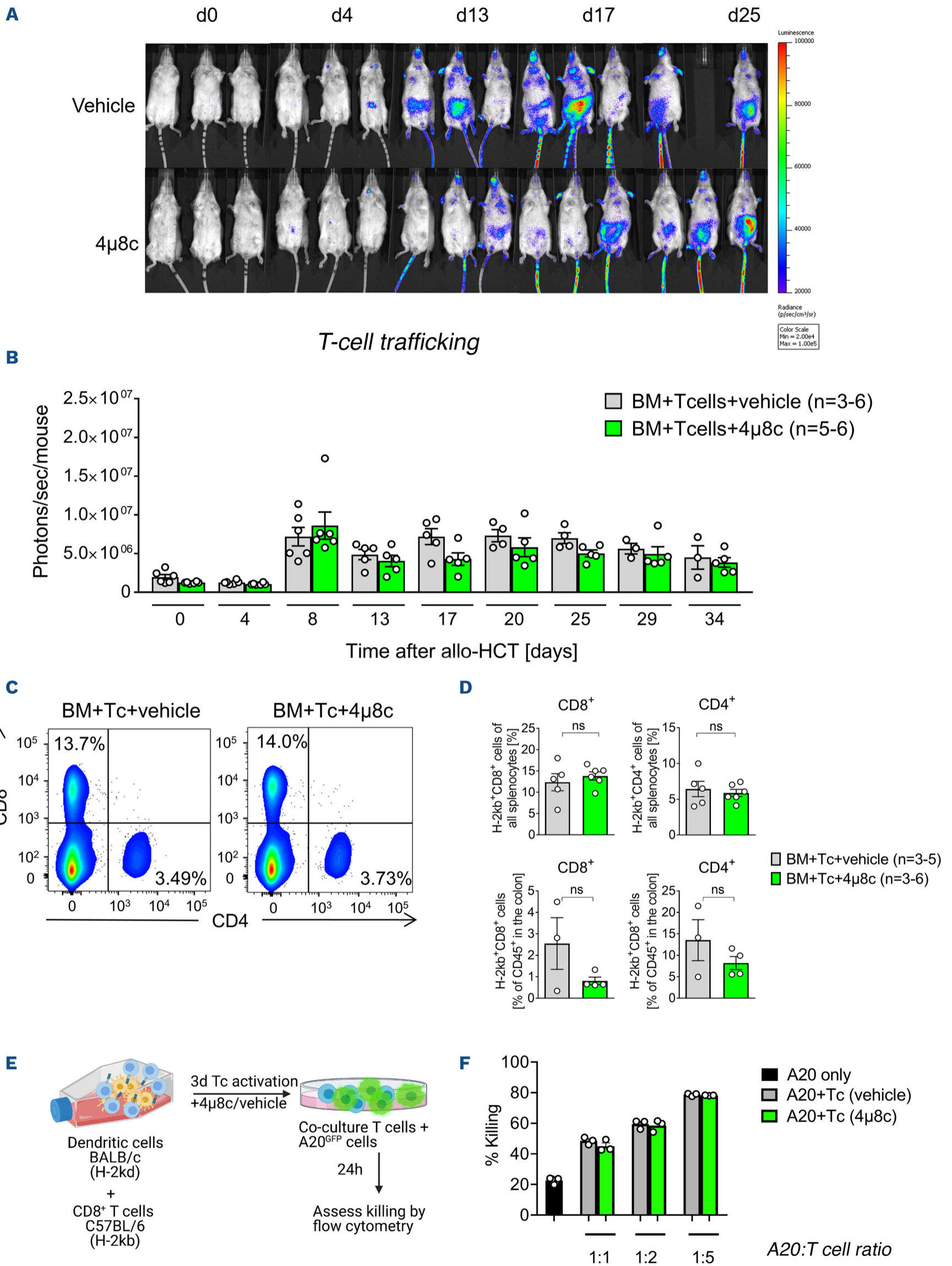


Figure 7. IRE1 α inhibition does not impair thymic and peripheral blood regeneration. (A-E) BALB/c mice underwent transplantation and were treated with 4 μ 8c as described in Figure 6A. On day 14 and day 29 after allogeneic hematopoietic cell transplantation (allo-HCT), leukocyte subpopulations and phenotype in the peripheral blood was analyzed. In addition, thymus reconstitution was assessed on day 29. Data were pooled from n=4 mice in the untreated group and n=9 mice each for the other groups. Each dot represents a single mouse. *P*-values were calculated using the two-tailed unpaired Student's *t*-test. ns: not significant. (A) Schematic overview of the experiment, created with BioRender.com. (B) Hemoglobin, platelet and white blood cell count including differentiation into granulocytes, monocytes and lymphocytes from mice treated as shown in (A). (C) Percentages of leukocyte subpopulations assessed by flow cytometry. Pre-gating on single cells – living cells – CD45⁺ was performed. Neutrophils were defined as CD11b⁺ Ly6G⁺. Monocytes were defined as CD11b⁺ Ly6G⁻. (D) Percentages of double positive (DP, CD4⁺CD8⁺), single CD4⁺, single CD8⁺ and double negative (DN, CD4⁻CD8⁻) T cells in the thymus of recipient mice. Pre-gating on single cells- living cells – CD45⁺ – CD3⁺ was performed. (E) Percentages of medullary thymic epithelial cells (mTEC, CD45⁻ EpCAM⁺ Ly51⁺), cortical thymic epithelial cells (cTEC, CD45⁻ EpCAM⁺ Ly51⁻) and fibroblasts (CD45⁻CD140⁺) in the thymus of recipient cells. Pre-gating on single cells and living cells was performed.



Continued on following page.

Figure 8. IRE1 α inhibitor treatment does not affect alloreactive T-cell expansion. (A, B) BALB/c mice underwent transplantation as described in Figure 6A using luciferase-transgenic T cells. (A) Representative bioluminescence (BLI) images from several time points. (B) Quantification of the BLI measurement is shown. Signal was quantified from the whole body in photons/sec/mouse. Data were pooled from n=6 mice/group. Each dot represents a single mouse. One representative result from three independent experiments is shown. (C, D) Flow cytometry analysis of T cells isolated from recipient spleens and colons on day 14 after allogeneic hematopoietic cell transplantation (allo-HCT) (C57BL/6 in BALB/c model). (C) Representative flow cytometry dot plots from the spleen are shown. (D) Combined data pooled from n=5-6 mice/group for the percentage of donor CD4⁺ and CD8⁺ T cells in the spleen (upper panel) and colon lamina propria (lower panel). Each dot represents a single mouse. One representative result from two independent experiments is shown. *P*-values were calculated using the two-tailed unpaired Student's *t*-test. ns: not significant. (E) C57BL/6 CD8⁺ T cells were activated in a co-culture with allogeneic BALB/c bone marrow-derived dendritic cells in the presence or absence of 5 μ M 4 μ 8c for 72 hours (h). CD8⁺ T cells were then incubated with GFP⁺ A20 lymphoma cells and the percentage of dead cells after 24 h of culture was assessed by flow cytometry. Schematic overview created with BioRender.com. (F) Percentage of dead A20 cells alone or at three different co-culture ratios with CD8⁺ T cells activated as described in (E). The experiment was repeated three times with four or five replicates each. One representative result is shown.

duced cell death in intestinal organoids with an increased release of the DAMP uric acid. Production of uric acid as a consequence of tissue damage during the conditioning treatment has been shown to promote GvHD by activating antigen-presenting cells.^{20,21} Short-term ER stress induces a stress-associated transcriptomic reprogramming with genes related to cellular signaling, expression regulation, metabolism, the cytoskeleton and others being upregulated.³³ Among these are multiple inflammation-associated genes, in particular chemokines, cytokines and acute phase proteins.³³ Higher expression of these mediators due to chronic activation of the UPR might perpetuate the tissue damage during GvHD by supporting the characteristic inflammatory microenvironment of the disease.

Deletion of *Xbp1* led to a global dysregulation of the UPR in mice developing GvHD and was associated with a significantly decreased survival rate and increased GvHD histopathology. In a preclinical model of liver injury, mice with liver-specific deletion of *Xbp1* showed initially a similar UPR activation after chemical ER stress induction with tunicamycin when compared to wild-type animals. However, this activation was significantly prolonged indicating the development of chronic ER stress in these animals.³⁴ UPR dysregulation by *Xbp1* deletion changes the composition of the intestinal epithelium. Previous studies by Kaser et al. show that mice with a *Xbp1* deletion in the intestinal epithelium had a loss of Paneth and goblet cells with rising age while at the same time intestinal stem cells and transit-amplifying cells appeared increased.^{17,35} Upon GvHD induction, a loss of Paneth cell occurs and its severity is a predictive marker of GvHD outcome.^{22,36,37} In our study, this loss was more pronounced in animals with a selective deletion of *Xbp1* with multiple defensin subtypes, which are produced by Paneth cells, being amongst the most differentially regulated genes in *Xbp1* ^{Δ IEC} mice. One additional mechanism by which ER stress might modulate intestinal inflammation is by altering the microbiome. The microbiome has become increasingly important for the understanding of GvHD pathology. Several studies in mice and humans show that GvHD severity and mortality are correlated with reduced microbial diversity and a shift from protective towards det-

rimental bacterial species.^{38,39} A protective role has been shown for the phylum Firmicutes and specifically for members of the Clostridia class.^{24,25} The beneficial effects of these bacteria could be attributed to the generation of anti-inflammatory metabolites, such as short-chain fatty acids. To the best of our knowledge, this study is the first one to describe the intestinal microbiome composition in *Xbp1* ^{Δ IEC} mice. We observed that these mice have reduced abundance of Firmicutes compared to their wild-type littermates. In particular, the Clostridia class including the Lachnospiraceae family were decreased. These changes closely resemble the changes observed during GvHD induction. One possible explanation for this dysbiosis is, that the intestinal environment is changed due to the reduced numbers of Paneth cells, and the lower concentrations of their anti-microbial products, defensins, lysozyme and Reg3 γ . In our view, these data support the hypothesis that there are pre-existing changes in the microbiome in *Xbp1* ^{Δ IEC} mice that predispose to GvHD development.

The UPR provides multiple targets for signaling modulation by inhibition of specific branches. We proposed that specific UPR signaling inhibition might aid in modulating ER stress signaling from pro-apoptotic to cell-protective pathways. Here, we used 4 μ 8c and B-I09, inhibitors of IRE1 α RNase activity, and GSK2606414 as a PERK inhibitor. Administration of IRE1 α inhibitors, but not the PERK inhibitor, showed a beneficial effect in GvHD-developing mice. Mechanistically, 4 μ 8c decreased TNF-associated intestinal cell death. A crosstalk between IRE1 α and TNF signaling has been documented previously.⁴⁰ ER stress can induce the expression of various pro-inflammatory cytokines.⁴¹ Indeed, administration of 4 μ 8c in a murine model of rheumatoid arthritis decreased disease severity by blocking pro-inflammatory cytokine secretion.⁴² At the same time, TNF is known to induce ER stress.⁴³ It is conceivable that pro-apoptotic UPR employs at least in part the same pathways as TNF signaling so that inhibition of IRE1 α can ameliorate the cytotoxic effects of both. Interestingly, 4 μ 8c showed a higher protective effect in GvHD animals, compared to B-I09. These differences might be due to variations in bioavailability after intraperitoneal injection. Another potential consideration would be

their specificity. Both compounds have been developed as potent and specific inhibitors of IRE1 α RNase activity, and little is known about potential off-target effects. In a previous study, 4 μ 8c was reported to have anti-oxidant capacity in endothelial and pancreatic cells by inhibiting xanthine/xanthine oxidase-catalyzed superoxide production and angiotensin II-induced ROS production.⁴⁴ In light of this report, it is conceivable that 4 μ 8c has combined beneficial effects in GvHD due to IRE1 α inhibition, and an anti-oxidative effect, which makes it a particularly interesting compound for further testing.

Besides having influence on signaling in intestinal cells, systemic IRE1 α inhibition might potentially have effects on immune cell reconstitution and immune responses against pathogens and malignant cells. Our data show that 4 μ 8c did neither cause alterations in platelet and hemoglobin recovery, nor on lymphocyte differentiation and effector memory development. Furthermore, we did not observe a change in T-cell expansion and cytokine production upon administration of 4 μ 8c. The capacity to kill A20 lymphoma cells was also not affected. These data are in line with previous reports, showing that dendritic cells, which were activated in the presence of the IRE1 α inhibitor B-109, were capable of eliciting strong anti-tumor responses in T cells.⁴⁵ In addition, a direct anti-tumor effect of B-109 against chronic lymphocytic leukemia cells has been reported.⁴⁶ Interestingly, specific inhibition of IRE1 α significantly inhibited influenza A viral replication in cell lines.⁴⁷ In light of these publications, our results provide encouraging evidence that 4 μ 8c treatment might spare anti-viral and anti-tumor responses while diminishing GvHD severity, even though further *in vivo* studies are necessary to provide additional confirmation.

Contrary to acute GvHD pathogenesis, donor B cells play an essential role in the context of chronic GvHD. These cells secrete antibodies in high quantities and are therefore highly dependent on a properly functioning UPR and are sensitive to ER stress; additionally it was found that XBP1 is essential for plasma cell differentiation.⁴⁸ It is therefore conclusive that several attempts were made to target ER stress and the UPR in the setting of chronic GvHD. The administration of the IRE1 inhibitor B-109 was found to reduce clinical features in a cutaneous model of chronic GvHD, with infiltrations of the skin by donor T cells and dendritic cells being reduced.⁴⁹ In another study, the use of the chemical chaperone 4-phenylbutyric acid (4-PBA) led to the amelioration of chronic GvHD-induced fibrosis.³² Based on our data, we propose that excessive ER stress and the activation of the UPR are mechanisms which mediate tissue injury during intestinal GvHD. Our study provides the first evidence that administration of an IRE1 α inhibitor is a pharmacologi-

cal intervention that reduces intestinal GvHD in mice and should be considered for testing in GvHD patients.

Disclosures

RZ received speakers fees from Novartis, Incyte and Mallinckrodt.

Contributions

EH, RZ and PA developed the overall concept and designed research; EH, FMU, BS, DP, and PA conducted the experiments and analyzed data; GA and MB performed bioinformatics analysis; MK, MP and BG performed and analyzed 16S rRNA sequencing; ASG and KA developed and analyzed histological stains; PE, SM, NK and JD provided reagents and/or conceptual input; PA and RZ provided funding and supervision; EH and PA wrote the manuscript. All authors discussed the results and contributed to the final manuscript.

Acknowledgments

The authors would like to acknowledge Dr. L. Glimcher for providing the XBP1 flox/flox mice as a gift; Dr. D. Kaiserlian for providing the MODE-K cell line; Dr. H. Andrlova for providing protocols for experimental procedures; and K. Gräwe for performing immunohistochemical stainings.

Funding

PA was supported by the Else Kröner-Fresenius-Stiftung (EKFS 2015_A147 to PA), the German Cancer Consortium (DKTK, FR 01-375) and a scholarship from the Berta Ottenstein Program for Clinician Scientists, Faculty of Medicine, Medical Center – University of Freiburg, Germany. RZ is supported by the Deutsche Forschungsgemeinschaft (DFG): SFB1479 (Project ID: 441891347), SFB1160, TRR167 and SFB850, the INTERREG V European regional development fund (European Union) program (Project 3.2 TRIDIAG), the European Union: GVHDCure Proposal n° 681012 ERC consolidator grant, the Deutsche Krebshilfe (grant number 70113473), the Jose-Carreras Leukemia foundation (grant number DJCLS 01R/2019) and the Wilhelm Sander Stiftung (grant 2008.046.4). NK was supported by the German Research Foundation (DFG) under German's Excellence Strategy (CIBSS - EXC 2189 – Project ID 390939984). MB is supported by the Deutsche Forschungsgemeinschaft (DFG) – SFB 850 subprojects C9 and Z1, SFB1479 (Project ID: 441891347- S1), SFB1160 (Project Z02), SFB1453 (Project S1) and TRR167 (Project Z01), the German Federal Ministry of Education and Research by MIRACUM within the Medical Informatics Funding Scheme (FKZ 01ZZ1801B).

Data-sharing statement

Microarray data are available on GEO under accession number GSE156469 (with the token uhgrqykubhmppl).

References

1. Zeiser R, Blazar BR. Acute graft-versus-host disease - biologic process, prevention, and therapy. *N Engl J Med.* 2017;377(22):2167-2179.
2. Zeiser R. Advances in understanding the pathogenesis of graft-versus-host disease. *Br J Haematol.* 2019;187(5):563-572.
3. Köhler N, Zeiser R. Intestinal microbiota influence immune tolerance post allogeneic hematopoietic cell transplantation and Intestinal GVHD. *Front Immunol.* 2018;9:3179.
4. Malard F, Huang XJ, Sim JPY. Treatment and unmet needs in steroid-refractory acute graft-versus-host disease. *Leukemia.* 2020;34(5):1229-1240.
5. Lindemans CA, Calafiore M, Mertelsmann AM, et al. Interleukin-22 promotes intestinal-stem-cell-mediated epithelial regeneration. *Nature.* 2015;528(7583):560-564.
6. Zhang X, Liu S, Wang Y, et al. Interleukin22 regulates the homeostasis of the intestinal epithelium during inflammation. *Int J Mol Med.* 2019;43(4):1657-1668.
7. Takashima S, Kadowaki M, Aoyama K, et al. The Wnt agonist R-spondin1 regulates systemic graft-versus-host disease by protecting intestinal stem cells. *J Exp Med.* 2011;208(2):285-294.
8. Hayase E, Hashimoto D, Nakamura K, et al. R-Spondin1 expands Paneth cells and prevents dysbiosis induced by graft-versus-host disease. *J Exp Med.* 2017;214(12):3507-3518.
9. Norona J, Apostolova P, Schmidt D, et al. Glucagon-like peptide 2 for intestinal stem cell and Paneth cell repair during graft-versus-host disease in mice and humans. *Blood.* 2020;136(12):1442-1455.
10. Haring E, Uhl FM, Andrieux G, et al. Bile acids regulate intestinal antigen presentation and reduce graft-versus-host disease without impairing the graft-versus-leukemia effect. *Haematologica.* 2021;106(8):2131-2146.
11. Hetz C, Chevet E, Harding HP. Targeting the unfolded protein response in disease. *Nat Rev Drug Discov.* 2013;12(9):703-719.
12. Calfon M, Zeng H, Urano F, et al. IRE1 couples endoplasmic reticulum load to secretory capacity by processing the XBP-1 mRNA. *Nature.* 2002;415(6867):92-96.
13. Yoshida H, Matsui T, Yamamoto A, Okada T, Mori K. XBP1 mRNA is induced by ATF6 and spliced by IRE1 in response to ER stress to produce a highly active transcription factor. *Cell.* 2001;107(7):881-891.
14. Nishitoh H, Matsuzawa A, Tobiume K, et al. ASK1 is essential for endoplasmic reticulum stress-induced neuronal cell death triggered by expanded polyglutamine repeats. *Genes Dev.* 2002;16(11):1345-1355.
15. Urano F, Wang X, Bertolotti A, et al. Coupling of stress in the ER to activation of JNK protein kinases by transmembrane protein kinase IRE1. *Science.* 2000;287(5453):664-666.
16. Han D, Lerner AG, Vande Walle L, et al. IRE1alpha kinase activation modes control alternate endoribonuclease outputs to determine divergent cell fates. *Cell.* 2009;138(3):562-575.
17. Kaser A, Lee AH, Franke A, et al. XBP1 links ER stress to intestinal inflammation and confers genetic risk for human inflammatory bowel disease. *Cell.* 2008;134(5):743-756.
18. Holtan SG, Shabaneh A, Betts BC, et al. Stress responses, M2 macrophages, and a distinct microbial signature in fatal intestinal acute graft-versus-host disease. *JCI Insight.* 2019;5(17):e129762.
19. Sato T, Clevers H. Primary mouse small intestinal epithelial cell cultures. *Methods Mol Biol.* 2013;945:319-328.
20. Wilhelm K, Ganesan J, Muller T, et al. Graft-versus-host disease is enhanced by extracellular ATP activating P2X7R. *Nat Med.* 2010;16(12):1434-1438.
21. Jankovic D, Ganesan J, Bscheider M, et al. The Nlrp3 inflammasome regulates acute graft-versus-host disease. *J Exp Med.* 2013;210(10):1899-1910.
22. Eriguchi Y, Takashima S, Oka H, et al. Graft-versus-host disease disrupts intestinal microbial ecology by inhibiting Paneth cell production of alpha-defensins. *Blood.* 2012;120(1):223-231.
23. Simms-Waldrup TR, Sunkersett G, Coughlin LA, et al. Antibiotic-induced depletion of anti-inflammatory Clostridia is associated with the development of graft-versus-host disease in pediatric stem cell transplantation patients. *Biol Blood Marrow Transplant.* 2017;23(5):820-829.
24. Jenq RR, Taur Y, Devlin SM, et al. Intestinal Blautia is associated with reduced death from graft-versus-host disease. *Biol Blood Marrow Transplant.* 2015;21(8):1373-1383.
25. Mathewson ND, Jenq R, Mathew AV, et al. Gut microbiome-derived metabolites modulate intestinal epithelial cell damage and mitigate graft-versus-host disease. *Nat Immunol.* 2016;17(5):505-513.
26. Wysocki CA, Burkett SB, Panoskaltzis-Mortari A, et al. Differential roles for CCR5 expression on donor T cells during graft-versus-host disease based on pretransplant conditioning. *J Immunol.* 2004;173(2):845-854.
27. Taylor PA, Ehrhardt MJ, Lees CJ, et al. Insights into the mechanism of FTY720 and compatibility with regulatory T cells for the inhibition of graft-versus-host disease (GVHD). *Blood.* 2007;110(9):3480-3488.
28. Kennedy GA, Varelias A, Vuckovic S, et al. Addition of interleukin-6 inhibition with tocilizumab to standard graft-versus-host disease prophylaxis after allogeneic stem-cell transplantation: a phase 1/2 trial. *Lancet Oncol.* 2014;15(13):1451-1459.
29. Zeiser R, von Bubnoff N, Butler J, et al. Ruxolitinib for glucocorticoid-refractory acute graft-versus-host disease. *N Engl J Med.* 2020;382(19):1800-1810.
30. Choi SW, Braun T, Chang L, et al. Vorinostat plus tacrolimus and mycophenolate to prevent graft-versus-host disease after related-donor reduced-intensity conditioning allogeneic haemopoietic stem-cell transplantation: a phase 1/2 trial. *Lancet Oncol.* 2014;15(1):87-95.
31. Joly AL, Deepti A, Seignez A, et al. The HSP90 inhibitor, 17AAG, protects the intestinal stem cell niche and inhibits graft versus host disease development. *Oncogene.* 2016;35(22):2842-2851.
32. Mukai S, Ogawa Y, Urano F, Kudo-Saito C, Kawakami Y, Tsubota K. Novel treatment of chronic graft-versus-host disease in mice using the ER stress reducer 4-phenylbutyric acid. *Sci Rep.* 2017;7:41939.
33. Tsalikis J, Pan Q, Tattoli I, et al. The transcriptional and splicing landscape of intestinal organoids undergoing nutrient starvation or endoplasmic reticulum stress. *BMC Genomics.* 2016;17(1):680.
34. Olivares S, Henkel AS. Hepatic Xbp1 gene deletion promotes endoplasmic reticulum stress-induced liver injury and apoptosis. *J Biol Chem.* 2015;290(50):30142-30151.
35. Niederreiter L, Fritz TM, Adolph TE, et al. ER stress transcription factor Xbp1 suppresses intestinal tumorigenesis and directs intestinal stem cells. *J Exp Med.* 2013;210(10):2041-2056.
36. Levine JE, Huber E, Hammer ST, et al. Low Paneth cell numbers at onset of gastrointestinal graft-versus-host disease identify patients at high risk for nonrelapse mortality. *Blood.* 2013;122(8):1505-1509.
37. Eriguchi Y, Nakamura K, Hashimoto D, et al. Decreased secretion

- of Paneth cell alpha-defensins in graft-versus-host disease. *Transpl Infect Dis.* 2015;17(5):702-706.
38. Holler E, Butzhammer P, Schmid K, et al. Metagenomic analysis of the stool microbiome in patients receiving allogeneic stem cell transplantation: loss of diversity is associated with use of systemic antibiotics and more pronounced in gastrointestinal graft-versus-host disease. *Biol Blood Marrow Transplant.* 2014;20(5):640-645.
39. Taur Y, Jenq RR, Perales MA, et al. The effects of intestinal tract bacterial diversity on mortality following allogeneic hematopoietic stem cell transplantation. *Blood.* 2014;124(7):1174-1182.
40. Hu P, Han Z, Couvillon AD, Kaufman RJ, Exton JH. Autocrine tumor necrosis factor alpha links endoplasmic reticulum stress to the membrane death receptor pathway through IRE1alpha-mediated NF-kappaB activation and down-regulation of TRAF2 expression. *Mol Cell Biol.* 2006;26(8):3071-3084.
41. Bettigole SE, Glimcher LH. Endoplasmic reticulum stress in immunity. *Annu Rev Immunol.* 2015;33:107-138.
42. Qiu Q, Zheng Z, Chang L, et al. Toll-like receptor-mediated IRE1alpha activation as a therapeutic target for inflammatory arthritis. *EMBO J.* 2013;32(18):2477-2490.
43. Denis RG, Arruda AP, Romanatto T, et al. TNF-alpha transiently induces endoplasmic reticulum stress and an incomplete unfolded protein response in the hypothalamus. *Neuroscience.* 2010;170(4):1035-1044.
44. Chan SMH, Lowe MP, Bernard A, Miller AA, Herbert TP. The inositol-requiring enzyme 1 (IRE1alpha) RNase inhibitor, 4micro8C, is also a potent cellular antioxidant. *Biochem J.* 2018;475(5):923-929.
45. Betts BC, Locke FL, Sagatys EM, et al. Inhibition of human dendritic cell ER stress response reduces T cell alloreactivity yet spares donor anti-tumor immunity. *Front Immunol.* 2018;9:2887.
46. Tang CH, Ranatunga S, Kriss CL, et al. Inhibition of ER stress-associated IRE-1/XBP-1 pathway reduces leukemic cell survival. *J Clin Invest.* 2014;124(6):2585-2598.
47. Hassan IH, Zhang MS, Powers LS, et al. Influenza A viral replication is blocked by inhibition of the inositol-requiring enzyme 1 (IRE1) stress pathway. *J Biol Chem.* 2012;287(7):4679-4689.
48. Reimold AM, Iwakoshi NN, Manis J, et al. Plasma cell differentiation requires the transcription factor XBP-1. *Nature.* 2001;412(6844):300-307.
49. Schutt SD, Wu Y, Tang CH, et al. Inhibition of the IRE-1alpha/XBP-1 pathway prevents chronic GVHD and preserves the GVL effect in mice. *Blood Adv.* 2018;2(4):414-427.